JACS
JOURNAL OF THE AMERICAN CHEMICAL SOCIETY

COMMUNICATION

pubs.acs.org/JACS

Molecular Logic Gates Using Surface-Enhanced Raman-Scattered Light

Edward H. Witlicki,[†] Carsten Johnsen,[‡] Stinne W. Hansen,[‡] Daniel W. Silverstein,[∥] Vincent J. Bottomley,[†] Jan O. Jeppesen,[‡] Eric W. Wong,[§] Lasse Jensen,[∥] and Amar H. Flood*[,†]

[†]Chemistry Department, Indiana University, 800 East Kirkwood Avenue, Bloomington, Indiana 47405, United States

[‡]Department of Physics and Chemistry, University of Southern Denmark, Campusvej 55, DK-5230 Odense M, Denmark

[§]Department of Chemistry, The Pennsylvania State University, University Park, Pennsylvania 16802, United States

[∥]Etamota Corporation, 2665-D Park Center Drive, Simi Valley, California 93065, United States

Supporting Information

ABSTRACT: A voltage-activated molecular-plasmonics device was created to demonstrate molecular logic based on resonant surface-enhanced Raman scattering (SERS). SERS output was achieved by a combination of chromophore−plasmon coupling and surface adsorption at the interface between a solution and a gold nanodisc array. The chromophore was created by the self-assembly of a supramolecular complex with a redox-active guest molecule. The guest was reversibly oxidized at the gold surface to the +1 and +2 oxidation states, revealing spectra that were reproduced by calculations. State-specific SERS features enabled the demonstration of a multigate logic device with electronic input and optical output.

Molecular logic gates[1] are prototypes of miniaturized information processing units that can be utilized in a variety of environments ranging from solution-phase[1] to solid-state devices.[2] The basic criteria for the operation of molecule-based logic gates[3] are (1) fast and observable responses (output) that result from external stimuli (input) and (2) adequate reversibility for resetting and reuse. Supramolecular chemistry offers several key advantages toward fulfilling these requirements.[3] For instance, many colored charge-transfer (CT) complexes[4] can be rapidly and reversibly changed using electrochemical stimuli. Here we consider a new optical output based on the inelastic scattering of laser light, i.e., surface-enhanced Raman scattering (SERS),[5] where molecular logic arises from the redox activity of a supramolecular system.

This work was partially inspired by recent accounts of optical information being carried along metallic wires as plasmons, i.e., as light propagating along the surface of a wire.[6] These surface plasmon resonances (SPRs) support large electric fields that confer high degrees of enhancement to SERS spectra. Thus, information can potentially be transported using near-field light (plasmons)[6] and then transmitted into the far field as Raman-scattered photons. Computational logic can be implemented by employing the metallic nanostructures as electrodes. Voltage can serve as the input to redox-active molecules, with signal output as a SERS spectrum. To the best of our knowledge, no molecular logic systems using SERS have been devised to date; therefore, we describe a proof-of-principle system that can be considered as an active molecular plasmonics device for elementary computation.

A color-matching strategy[7] was employed to achieve resonance (Figure 1) between a supramolecular (Figure 1a) or molecular (Figure 1b,c) chromophore, the SPR (Figure 1d), and the laser light (785 nm; red arrow in Figure 1). When these spectral features are all in alignment, *resonant* SERS (also labeled SERRS) is achieved by the mechanism of chromophore−plasmon coupling.[9] We have shown previously[8,10] that this approach works when plasmonically active gold nanodisc arrays (Figure 1d, right) are interfaced with solutions of the supramolecular complex[11] formed between the tetracationic cyclophane host cyclobis(paraquat-*p*-phenylene) ($CBPQT^{4+}$)[12] and a tetrathiafulvalene (TTF) guest molecule. Here, our active guest makes use of a monopyrrolo-TTF (MPTTF)[13] derivative to generate (Figure 1a) a green-colored CT complex in the form of the [2]pseudorotaxane $MPTTF\subset CBPQT^{4+}$. The MPTTF guest displays two reversible one-electron redox processes[14] that form $MPTTF^{+}$ and $MPTTF^{2+}$ with concomitant disassembly of the complex. Electrostatic repulsion between the cations and the tetracationic $CBPQT^{4+}$ host reversibly drives this process.[11] Concomitantly, different chromophores characteristic[15] of the oxidized MPTTF states (Figure 1b,c for $MPTTF^{+}$ and $MPTTF^{2+}$, respectively) are generated. The new chromophores have varying degrees of overlap with the SPR, thus generating different SERS (output) signals.

To test this idea, the SERS spectra from the complex and its oxidized states were recorded (Figure 2) by incorporating the gold-coated nanoarray into a three-electrode cell using a Pt counter electrode and a Ag/AgCl pseudoreference electrode.[13] Raman spectra were collected from a thin solution film (<1 μm) of the complex (186 μM, MeCN)[7,13] interfaced with the nanoarray. At 0.0 V, a resonant SERS spectrum from the complex was observed (Figure 2, green trace) with a characteristic band at 1640 cm^{-1}.[8] At oxidizing potentials, spectra for the cations $MPTTF^{+}$ (+0.6 V) and $MPTTF^{2+}$ (+0.9 V) were obtained (Figure 2, red and blue traces, respectively). These data agree with published accounts of the SERS spectra of the parent TTF cations.[16] The strong bands for $MPTTF^{+}$ at 508 cm^{-1} and $MPTTF^{2+}$ at 529 cm^{-1} dominate the spectra. These two bands together with the 1640 cm^{-1} band for the complex are specific for each state of the logic device.

Received: February 1, 2011
Published: April 21, 2011

dx.doi.org/10.1021/ja200992x | *J. Am. Chem. Soc.* 2011, 133, 7288–7291

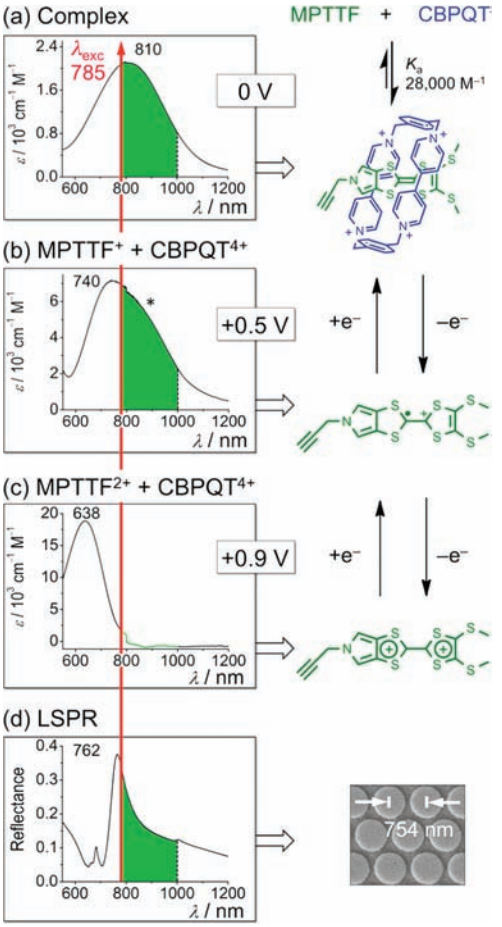

Figure 1. (a) Recognition between MPTTF and CBPQT^{4+} results in a colored complex.[7] (b, c) Oxidation to the (b) MPTTF^{+} and (c) MPTTF^{2+} cations generates different chromophores. (d) Reflectance spectrum (air) from a gold nanodisc array (shown in the SEM image). The spectral overlap for the Raman scattering is in green, and the red arrow indicates the wavelength of the laser light. Conditions: 1 mM CBPQT^{4+} + 2 equiv of MPTTF, 0.1 M $TBAPF_6$, potentials vs Ag/AgCl, MeCN solvent, 298 K.

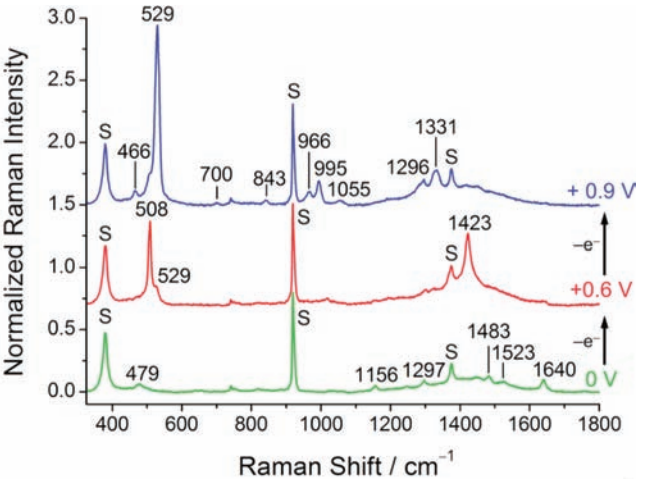

Figure 2. Experimental SERS spectra for the MPTTF⊂CBPQT^{4+} complex (green line), singly oxidized MPTTF^{+} + CBPQT^{4+} (red line), and doubly oxidized MPTTF^{2+} + CBPQT^{4+} (blue line) obtained at the solution−nanoarray interface. Conditions: λ_{exc} = 785 nm (10 s, 30 mW, average of 10 scans); 600 μM CBPQT^{4+} + 200 μM MPTTF (186 μM MPTTF⊂CBPQT^{4+});[7] controlled electrolysis, 0.1 M $TBAPF_6$, MeCN solvent, 298 K; S = solvent peak.

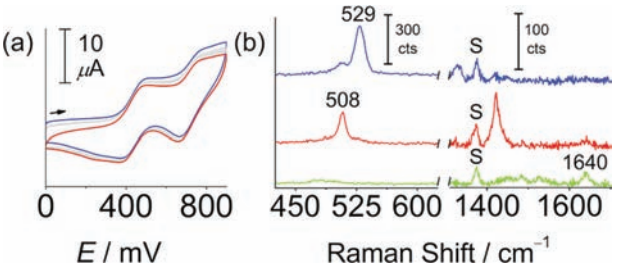

Figure 3. (a) Overlay of 40 consecutive CVs and (b) averages of 40 SERS spectra in the 0.0 V (green), ~0.6 V (red), and ~0.9 V (blue) spectral windows. Conditions: ν = 50.5 mV s^{-1}, λ_{exc} = 785 nm (2.8 s, 30 mW; average of 40 spectra); also see the caption of Figure 2.

As a means to examine the possibility of real-time monitoring as well as the system's reversibility and reproducibility, SERS spectra were collected during 40 consecutive cyclic voltammograms (CVs) [scan rate (ν) = 50.5 mV s^{-1}; Figure 3a].[17] The spectra obtained (Figure 3b) are representative of the species generated at the electrode surface by comparison to controlled electrolysis experiments (Figure 2). The similarity of the consecutive CVs (Figure 3a) over the course of 40 scans attests to the reversibility and stability. This situation allowed spectra recorded for only 2.8 s at ~0, ~0.6, and ~0.9 V during the 40 CVs to be averaged together (Figure 3b).

When the current (I) and SERS intensities from the CV cycling experiment were plotted against time (Figure 4), they correlated well with each other. In the high-wavenumber region, the CBPQT^{4+}-based band[8] at 1640 cm^{-1}, which is a signature for the complex, was present at 0.0 V. This band disappeared during the voltage ramp (Figure 4, top) as the band associated with MPTTF^{+} (508 cm^{-1}) increased, concomitant with the first oxidation (+0.5 V, 9.8 s). This signature gave way with the onset of the second oxidation (+0.75 V, 14.8 s) to the characteristic MPTTF^{2+} band (529 cm^{-1}). During the return ramp (0.9 to 0 V), the Raman bands associated with the three species showed a smooth change from one to the other in the reverse of the order seen in the forward sweep. It is these correlated voltage inputs and SERS outputs that provide the basis for logic.

It is important to note that the scattering bands for MPTTF^{+} (508 cm^{-1}) and MPTTF^{2+} (521 cm^{-1}) are very close in wavelength (819.01 and 817.60 nm, respectively), creating a situation in which cross-talk effects can occur. However, the resolving power of the spectrometer in this case (less than ±1 cm^{-1} or ±0.07 nm) was sufficient to mitigate cross-talk effects, even in the situation where the two bands had the same intensity during the oxidation from the monocation to the dication (Figure 4, where the blue and red traces intersect).[13]

The voltage-gated interconversions (Figure 4) provide a set of voltage inputs and optical outputs that can be utilized to identify representative logic gates.[19] The potentials of 0, +0.6, and +1.2 V can be represented as a battery series with the inputs 0x, 1x, and 2x, where x = +0.6 V (the experiments used +0.9 V, but +1.2 V gave the same response).[13] The vibrational bands in the SERS spectra for the three oxidation states can be considered as three output channels expressed as either Raman shift positions (cm^{-1})

dx.doi.org/10.1021/ja200992x | J. Am. Chem. Soc. 2011, 133, 7288–7291

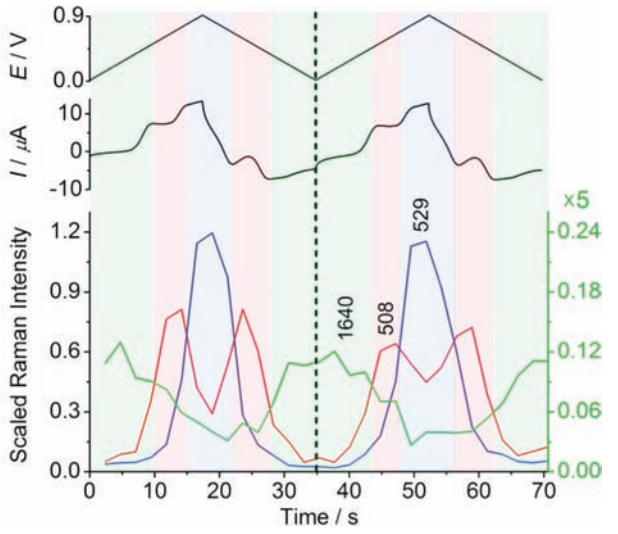

Figure 4. Coupled current (middle) and Raman (bottom) signals collected from the nanodisc array during in situ CV ramps (top). The Raman intensities correspond to the MPTTF⊂CBPQT^{4+} complex (1640 cm^{-1}, green trace),[18] MPTTF^{+} (508 cm^{-1}, red trace), and MPTTF^{2+} (529 cm^{-1}, blue trace). Conditions: same as for Figure 3.

relative to the excitation wavelength or as absolute wavelengths (nm): 1640 cm^{-1} (901 nm), 508 cm^{-1} (818 nm), and 529 cm^{-1} (819 nm). At 0*x* (0 V), where the inputs are *A* = *B* = 0, the MPTTF⊂CBPQT^{4+} complex dominates the spectrum, giving the output light at 901 nm. At 1*x* (+0.6 V), one electron is removed to create the MPTTF^{+} state. In this case, the inputs are *A* = 1, *B* = 0 or *A* = 0, *B* = 1, each representing the first oxidation and giving the output light at 818 nm. Lastly, at 2*x* (+1.2 V), where *A* = *B* = 1, the second oxidation occurs with light scattered at 819 nm. This configuration allows any one of three different logic gates to be active, depending on the wavelength of light being monitored. The I/O truth table (Figure 5) shows that information is processed as a NOR, XOR, or AND gate when 901, 818, or 819 nm light, respectively, is monitored. Multiple logic gates can be used concurrently by monitoring two or more of these wavelengths simultaneously.

We believe that the SERS output was achieved when all of the elements (plasmonically active electrode, chromophores, and input laser light) were brought together into one integrated device. To support this idea, the signal enhancement mechanisms were examined. For this purpose, the SERS spectra were compared to the solution-phase data[13] for each state. The spectrum of the MPTTF⊂CBPQT^{4+} complex (Figure 2) can be assigned as a SERRS spectrum on the basis of the fact that it resembles the *resonance* Raman spectrum of the bulk solution.[13] The SERRS spectrum is almost identical to the spectrum generated from the complex with the parent TTF under the same surface-enhanced conditions,[8] a characteristic difference being the presence of a new vibration at 1523 cm^{-1}. This band is attributed to the pyrrolo moiety. The surface Raman spectrum originating from the MPTTF^{+} monocation (Figure 2b) is also consistent with resonance (i.e., SERRS) on the basis of a comparison with solution data.[13] In both cases, the SERS intensity is enhanced relative to bulk solution, consistent with enhancement by coupling to the SPR.

The SERS spectrum of the MPTTF^{2+} dication (Figure 2) shows a greatly enhanced signal even though its chromophore (Figure 1c) has poor spectral overlap with the plasmon (Figure 1d).

x (MPTTF oxidation state)	Input Values *A*	*B*	NOR 1640 cm^{-1} (901 nm)	XOR 508 cm^{-1} (818 nm)	AND 529 cm^{-1} (819 nm)
0*x* (0)	0	0	1	0	0
1*x* (+1)	1 0	0 1	0	1	0
2*x* (+2)	1	1	0	0	1

Figure 5. Truth table representing the optical output of the MPTTF⊂CBPQT^{4+} system (*x* = +0.6 V).

This observation is consistent with the solution spectrum of this dication and the simulated normal Raman spectrum.

The surface-enhanced vibrational bands of all species are shifted to lower wavenumbers relative to solution.[13] This observation verifies that the enhancement of the SERS spectra also originates from surface adsorption, which would place each species inside the most intense part of the electric field of the SPR.[20,21]

To gain further understanding of the SERS spectra, we simulated the resonance Raman spectra (see the Supporting Information) for the MPTTF⊂CBPQT^{4+} complex and the MPTTF^{+} and MPTTF^{2+} cations using the time-dependent theory of Raman scattering and long-range corrected functionals.[13,22] These functionals were found to be essential to correctly describe the excited states of the MPTTF⊂CBPQT^{4+} complex and its oxidized forms.[13]

In general, there was reasonable agreement between the simulated and experimental spectra,[13] making an assignment possible. The simulations showed that the state-specific vibrations 1640 (complex), 508 (monocation), and 529 cm^{-1} (dication) involve bonds whose lengths change with electronic excitation.[13] Consistently, these vibrations show strong resonance enhancement.[13] In addition, the 508 cm^{-1} band in MPTTF^{+} is enhanced by vibronic coupling to the strong band at 1423 cm^{-1}, as evidenced by the overtone at 1930 cm^{-1} in the solution resonance Raman and SERRS spectra.[13] This vibronic coupling can also be seen in the experimental absorption spectrum for MPTTF^{+}, where the separation between the main band and the shoulder (marked by * in Figure 1b) is on the order of 1460 cm^{-1}. The worst agreement with experiment was found for the MPTTF^{2+} dication, where the relative intensity of the vibrational band at 529 cm^{-1} was underestimated relative to the experimental spectrum. This discrepancy is attributed to preresonance enhancements that occurred under the experimental conditions because this vibrational band is already strong in the normal Raman spectrum.[13]

Considerations of these signal enhancement mechanisms indicate the complexity of the solution−molecule−surface interfaces. Nevertheless, it is clear that the chromophore's resonance Raman spectrum is retained when on-resonance conditions are met in the SERS experiment. It is reasonable to expect that this behavior should not change substantially in a possible solid-state version and that good environmental stability would ensue using the system tested here. In studies using related molecules,[23] the electrochemical and spectroscopic behavior remained the same in the solution-phase and solid-state environments. Furthermore, temperature-dependence studies showed that while the reverse-switching kinetics slowed in the solid state,[24] both the forward and reverse-switching mechanisms remained the same.[25]

In summary, we have demonstrated a voltage-to-light logic device using Raman scattering of laser light by molecules interfaced with a plasmonically active nanoarray. Surface enhancement

dx.doi.org/10.1021/ja200992x |*J. Am. Chem. Soc.* 2011, 133, 7288–7291

of the signal originates from resonance of the chomophores with the surface plasmon and localization of the molecules/supermolecules inside the plasmon field by surface adsorption. Supramolecular chemistry provided a means of designing the active elements of this logic device in such a way that it is ultimately the actions of the molecular players that lead to the logic operations.

■ ASSOCIATED CONTENT

Supporting Information. General experimental methods, preparation of the MPTTF derivative, spectroscopy and characterization of the host−guest complexation, construction of the three-electrode cell, UV−vis−NIR spectroelectrochemistry of the MPTTF derivative, details of the simulations, and complete ref 11b. This material is available free of charge via the Internet at http://pubs.acs.org.

■ AUTHOR INFORMATION

Corresponding Author
aflood@indiana.edu

■ ACKNOWLEDGMENT

The authors acknowledge Indiana University for start-up funds (A.H.F.); the Strategic Research Council in Denmark (Project 2106-07-0031), the EC FP7 ITN "FUNMOLS" Project 212942, and the Villum Foundation for financial support (J.O.J.); the National Science Foundation (Grant CHE-0955689) (L.J.); and the National Aeronautics and Space Administration (NASA) for funds (E.W.W.). This work was supported in part through instrumentation funded by the National Science Foundation through Grant OCI-0821527.

■ REFERENCES

(1) (a) de Silva, A. P.; Gunaratne, H. Q. N.; McCoy, C. P. *Nature* **1993**, *364*, 42. (b) Asakawa, M.; Ashton, P. R.; Balzani, V.; Credi, A.; Mattersteig, G.; Matthews, O. A.; Montalti, M.; Spencer, N.; Stoddart, J. F.; Venturi, M. *Chem.—Eur. J.* **1997**, *3*, 1992. (c) Credi, A.; Balzani, V.; Langford, S. J.; Stoddart, J. F. *J. Am. Chem. Soc.* **1997**, *119*, 2679. (d) de Silva, A. P.; McClenaghan, N. D. *Chem.—Eur. J.* **2004**, *10*, 574.

(2) (a) Collier, C. P.; Mattersteig, G.; Wong, E. W.; Luo, Y.; Beverly, K.; Sampaio, K.; Raymo, F. H.; Stoddart, J. F.; Heath, J. R. *Science* **2000**, *289*, 1172. (b) Green, J. E.; Choi, J. W.; Boukai, A.; Bunimovich, Y.; Johnston-Halperin, E.; Delonno, E.; Luo, Y.; Sheriff, B. A.; Xu, K.; Shin, Y. S.; Tseng, H.-R.; Stoddart, J. F.; Heath, J. R. *Nature* **2007**, *445*, 414. (c) Kudernac, T.; Katsonis, N.; Browne, W. R.; Feringa, B. L. *J. Mater. Chem.* **2009**, *19*, 7168. (d) Angelos, S.; Yang, Y.-W.; Khashab, N. M.; Stoddart, J. F.; Zink, J. I. *J. Am. Chem. Soc.* **2009**, *131*, 11344.

(3) Raymo, F. M. *Adv. Mater.* **2002**, *14*, 401.

(4) Segura, J. L.; Martin, N. *Angew. Chem., Int. Ed.* **2001**, *40*, 1372.

(5) (a) Fleischman, M.; Hendra, P. J.; McQuillan, A. J. *Chem. Phys. Lett.* **1974**, *26*, 163. (b) Jeanmaire, D. L.; Van Duyne, R. P. *J. Electroanal. Chem.* **1977**, *84*, 1. (c) Albrecht, M. G.; Creighton, J. A. *J. Am. Chem. Soc.* **1977**, *99*, 5215.

(6) (a) Bozhevolnyi, S. I.; Volkov, V. S.; Devaux, E.; Laluet, J.-Y.; Ebbesen, T. W. *Nature* **2006**, *440*, 508. (b) Pala, R. A.; Shimizu, K. T.; Melosh, N. A.; Brongersma, M. L. *Nano Lett.* **2008**, *8*, 1506. (c) Zheng, Y. B.; Yang, Y.-W.; Jensen, L.; Fang, L.; Juluri, B. K.; Flood, A. H.; Weiss, P. S.; Stoddart, J. F.; Huang, T. J. *Nano Lett.* **2009**, *9*, 819.

(7) The concentrations used for these experiments were chosen in order to ensure >80% complexation based on $K_a = 28\,000\ M^{-1}$; see the Supporting Information for titrations with UV−vis−NIR and resonance Raman spectroscopy.

(8) Witlicki, E. H.; Andersen, S. S.; Hansen, S. W.; Jeppesen, J. O.; Wong, E. W.; Jensen, L.; Flood, A. H. *J. Am. Chem. Soc.* **2010**, *132*, 6099.

(9) (a) Haynes, C.; McFarland, A. D.; Van Duyne, R. P. *Anal. Chem.* **2005**, *77*, 339. (b) Dieringer, J. A.; McFarland, A. D.; Shah, N. C.; Stuart, D. A.; Whitney, A. V.; Yonzon, C. R.; Young, M. A.; Zhang, X.; Van Duyne, R. P. *Faraday Discuss.* **2006**, *132*, 9.

(10) Witlicki, E. H.; Hansen, S. W.; Christensen, M.; Hansen, T. S.; Nygaard, S. D.; Jeppesen, J. O.; Jensen, L.; Wong, E. W.; Jensen, L.; Flood, A. H. *J. Phys. Chem. A* **2009**, *113*, 9450.

(11) (a) Philp, D.; Slawin, A. M. Z.; Spencer, N.; Stoddart, J. F.; Williams, D. J. *J. Chem. Soc., Chem. Commun* **1991**, 1584. (b) Anelli, P. L.; *J. Am. Chem. Soc.* **1992**, *114*, 193. (c) Asakawa, M.; Dehaen, W.; L'abbé, G.; Menzer, S.; Nouwen, J.; Raymo, F. M.; Stoddart, J. F.; Williams, D. J. *J. Org. Chem.* **1996**, *61*, 9591. (d) Devonport, W.; Blower, M. A.; Bryce, M. R.; Goldenberg, L. M. *J. Org. Chem.* **1997**, *62*, 885. (e) Ashton, P. R.; Balzani, V.; Becher, J.; Credi, A.; Fyfe, M. C. T.; Mattersteig, G.; Menzer, S.; Nielsen, M. B.; Raymo, F. M.; Stoddart, J. F.; Venturi, M.; Williams, D. J. *J. Am. Chem. Soc.* **1999**, *121*, 3951. (f) Bryce, M. R.; Cooke, G.; Duclairoir, F. M. A.; Rotello, V. M. *Tetrahedron Lett.* **2001**, *42*, 1143. (g) Nielsen, M. B.; Jeppesen, J. O.; Lau, J.; Lomholt, C.; Damgaard, D.; Jacobsen, J. P.; Becher, J.; Stoddart, J. F. *J. Org. Chem.* **2001**, *66*, 3559.

(12) Odell, B.; Reddington, M. V.; Slawin, A. M. Z.; Spencer, N.; Stoddart, J. F.; Williams, D. J. *Angew. Chem., Int. Ed. Engl.* **1988**, *27*, 1547.

(13) See the Supporting Information.

(14) (a) Jeppesen, J. O.; Takimiya, K.; Jensen, F.; Becher, J. *Org. Lett.* **1999**, *1*, 1291. (b) Jeppesen, J. O.; Takimiya, K.; Jensen, F.; Brimert, T.; Nielsen, K.; Thorup, N.; Becher, J. *J. Org. Chem.* **2000**, *65*, 5794. (c) Jeppesen, J. O.; Becher, J. *Eur. J. Org. Chem.* **2003**, 3245.

(15) (a) Nygaard, S.; Laursen, B. W.; Flood, A. H.; Hansen, C. N.; Jeppesen, J. O.; Stoddart, J. F. *Chem. Commun* **2006**, 144. (b) Nygaard, S.; Leung, K. C.-F.; Aprahamian, I.; Ikeda, T.; Saha, S.; Laursen, B. W.; Kim, S.-Y.; Hansen, S. W.; Stein, P. C.; Flood, A. H.; Stoddart, J. F.; Jeppesen, J. O. *J. Am. Chem. Soc.* **2007**, *129*, 960.

(16) (a) Bozio, R.; Girlando, A.; Pecile, D. *Chem. Phys. Lett.* **1977**, *52*, 503. (b) Kuzmany, H.; Stolz, H. J. *J. Phys. C* **1977**, *10*, 2241. (c) Bozio, R.; Zanon, I.; Girlando, A.; Pecile, C. *J. Chem. Phys.* **1979**, *71*, 2282. (d) Siedle, A. R.; Candela, G. A.; Finnegan, T. F.; Van Duyne, R. P.; Cape, T.; Kokoszka, G. F.; Woyciejes, P. M.; Hashmall, J. A. *Inorg. Chem.* **1981**, *20*, 2635.

(17) The scan rate of 50.5 mV s^{-1} was chosen to synchronize the Raman spectrometer with the potentiostat during cyclic voltammetry.

(18) It should be noted that the green trace has been multiplied by a factor of 5 relative to the red and blue traces.

(19) Burch, C. *Logisim: A Graphical Tool for Designing and Simulating Logic Circuits*, version 2.6.1; http://ozark.hendrix.edu/~burch/logisim/ (accessed Feb 1, 2011).

(20) It is known that the cationic forms of the parent $TTF^{+/2+}$ cations are surface-active,[21] and therefore, surface-adsorption effects are also expected to be present for the monopyrrolo derivative.

(21) (a) Sandroff, C. J.; Weltz, D. A.; Chung, J. C.; Herschbach, D. R. *J. Phys. Chem.* **1983**, *87*, 2127. (b) Lu, T.; Cotton, T. M. *J. Phys. Chem.* **1987**, *91*, 5978. (c) Joy, V. T.; Srinivasan, T. K. K. *Chem. Phys. Lett.* **2000**, *328*, 221.

(22) (a) Tannor, D. J.; Heller, E. J. *J. Chem. Phys.* **1982**, *77*, 202. (b) Silverstein, D. W.; Jensen, L. *J. Chem. Theory Comput.* **2010**, *6*, 2845.

(23) (a) Steuerman, D. W.; Tseng, H.-R.; Peters, A. J.; Flood, A. H.; Jeppesen, J. O.; Nielsen, K. A.; Stoddart, J. F.; Heath, J. R. *Angew. Chem., Int. Ed.* **2004**, *43*, 6486. (b) Flood, A. H.; Wong, E. W.; Stoddart, J. F. *Chem. Phys.* **2006**, *324*, 280.

(24) Tseng, H.-R.; Wu, D.; Fang, N. X.; Zhang, X.; Stoddart, J. F. *ChemPhysChem* **2004**, *5*, 111.

(25) (a) Collier, C. P.; Jeppesen, J. O.; Luo, Y.; Perkins, J.; Wong, E. W.; Heath, J. R.; Stoddart, J. F. *J. Am. Chem. Soc.* **2001**, *123*, 12632. (b) Luo, Y.; Collier, C. P.; Jeppesen, J. O.; Nielsen, K. A.; Delonno, E.; Ho, G.; Perkins, J.; Tseng, H.-R.; Yamamoto, T.; Stoddart, J. F.; Heath, J. R. *ChemPhysChem* **2002**, *3*, 519.